ELSEVIER

Earth and Planetary Science Letters 181 (2000) 279–290

EPSL

www.elsevier.com/locate/epsl

Magnetic properties of aggregate polycrystalline diamond: implications for carbonado history

Günther Kletetschka [a,*], Patrick T. Taylor [a], Peter J. Wasilewski [b], Hugh G.M. Hill [b]

[a] *Geodynamics Branch, Code 921, NASA's Goddard Space Flight Center, Greenbelt, MD 20771 USA*
[b] *Astrochemistry Branch, Code 691, NASA's Goddard Space Flight Center, Greenbelt, MD 20771 USA*

Received 5 April 2000; received in revised form 20 June 2000; accepted 25 June 2000

Abstract

Carbonados are aggregate polycrystalline diamonds and are found in placer deposits of the Central African Republic (CAR) and the Bahia Province of Brazil. Their origin is uncertain, but several mutually exclusive hypotheses have been proposed, ranging from extraterrestrial to crustal, and mantle provenance. In an endeavor to further our understanding of these diamonds, we performed a series of magnetic characterization studies on 20 samples from the CAR. Our results reveal that the carbonados contain material with contrasting magnetic hysteresis behavior and magnetization. Acid leaching permitted us to monitor the distribution of magnetic carriers within the samples. An absence of sample size dependence on magnetization loss indicates that the magnetic carriers are distributed at the vitreous surface; including open pores and that the carbonado interior is essentially devoid of the magnetic carriers. The diamond's isolated non-magnetic interior of carbonados suggests that the initial formation environment was deficient in magnetic particles. The formation of the magnetic carriers is thus closely linked with the origin of the smooth surface, perhaps during the hypervelocity ejection of carbonados into the Earth's atmosphere. Partial ablation in the Earth's primordial, oxygen-poor atmosphere resulted in a fusion of the originally porous material and a decrease in the original pore density at the surface. Secondary mineralization of the impact-generated melt and/or the products of later diagenetic processes, containing the majority of the magnetic carriers, filled the remainder of the open pores. © 2000 Elsevier Science B.V. All rights reserved.

Keywords: diamond; carbonado; magnetic properties; impact features; magnetic hysteresis

1. Introduction

Carbonados are sintered polycrystalline micro-diamond aggregates with a porous, ceramic texture and a melt-like surface patina [1,2] (Fig. 1). The closed pores contain significant (up to 0.3 wt%) amounts of the total content of organic material of which 1% is in a form of polycyclic aromatic hydrocarbons (PAHs) [3]. The pores lack significant mantle mineral inclusions and are distinct from kimberlitic diamonds [1,4,5]. They have only been found in alluvial deposits in Bahia, Brazil, and in the Central African Republic (CAR).

* Corresponding author. Tel.: +1-301-286-8242; Fax: +1-301-286-0212; E-mail: gunther@denali.gsfc.nasa.gov

0012-821X/00/$ – see front matter © 2000 Elsevier Science B.V. All rights reserved.
PII: S0012-821X(00)00213-2

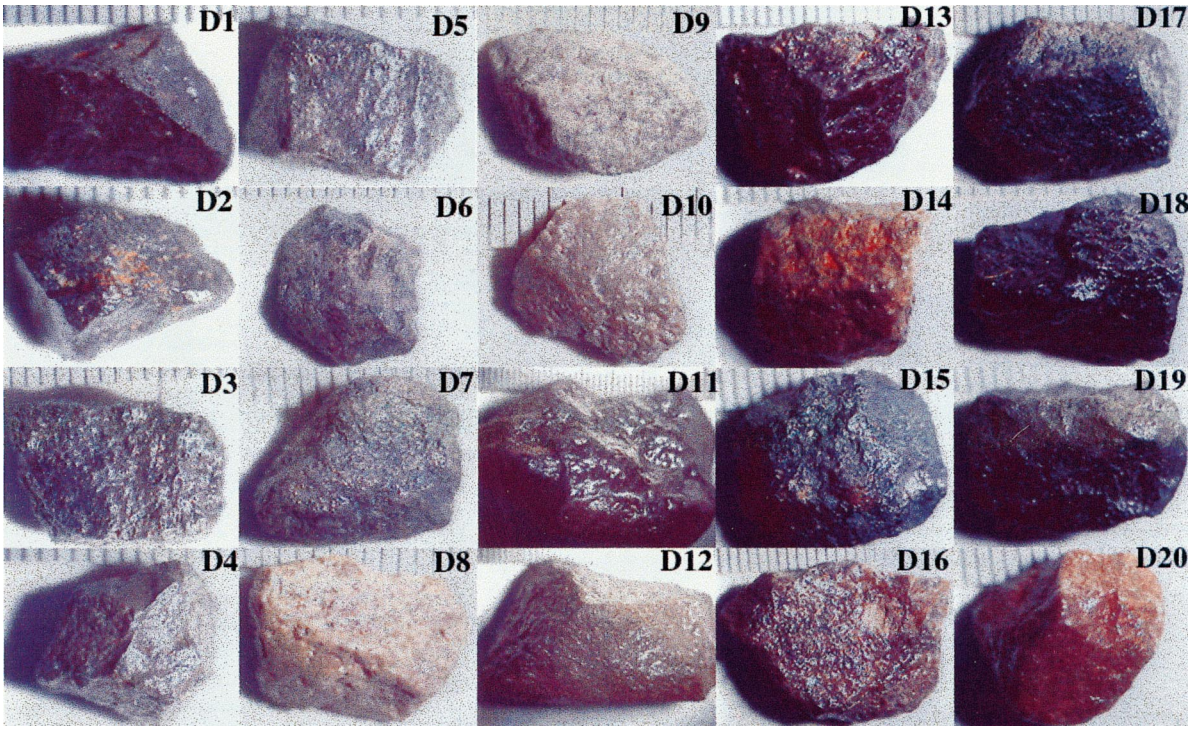

Fig. 1. Morphology and sizes of carbonado diamonds from Central Africa. The scale is marked by distance between the lines and is 1 mm.

These two areas may constitute a single source because they both lie on the West Congo–Salvador craton, only about 1500 km apart in a plate reconstruction of Gondwanaland [6]. These deposits are ~1.5 Ga old, while the carbonados are between 2.6 and 3.8 Ga [7]. Random orientation of the carbonado crystallites increases the structural integrity of the material with respect to the larger, single diamond crystals, which are subject to disintegration along cleavage planes. Precisely how the carbonado micro-crystals fused together and what mechanism caused the high porosity with trapped PAHs [3] is poorly understood, doubtless due to the fact that the origin of the carbonados is unclear.

Several carbonado genesis theories have been proposed. Robinson [8] proposed that formation in cold subduction slabs near continental margins could provide the high pressure and the organic-rich matter required for possible conversion into carbonado diamonds. A crustal origin is supported by the following isotopic and mineralogical data: Carbonados have light carbon (C) and helium (He) isotopic signatures [9,10]; contain an enrichment of light rare-earth elements (REEs) [9,11]; and have significant amounts of atmospheric noble gases [12]. They contain significant amounts of He, which appears to be inconsistent with the expected depletion of this element at mantle temperatures [4,13]. Carbonados also have high porosity with trapped organic material inside [3,5,14] which is incompatible with high-pressure mantle conditions [4].

An irradiation origin has also been proposed [12,15] based on the presence of high concentrations of parentless fission products (Xe, Kr) in both Brazilian and African carbonados. The rationale is that large amounts of fissiogenic species require uniform dispersion of U-rich material over geological time scales. The radiation associated with this material then contributes to the diamond formation mechanics [12].

An alternative mantle origin was proposed based on the similarity of the REE pattern in kimberlites and carbonados [16,17], the presence of nitrogen (N) platelets in the microcrystalline diamond (recorded by IR spectroscopy [16,18]) and low concentrations of syngenetic inclusions of rutile, ilmenite, and magnetite in the carbonado aggregates (characteristics, which are consistent with the mantle origin) [19].

A further hypothesis proposed that carbonados formed as a result of a primordial extraterrestrial bolide, impacting C-rich crustal sediments [20–23]. This diamond forming mechanism is often supported by the occurrence of the high-pressure deformation features and characteristic isotopic signatures, suggestive of a shock history [22].

Finally, Haggerty [4] proposed that carbonados are of extraterrestrial origin, based on the following evidence: the high abundance of C in the solar system; the existence of diamonds in primitive meteorites; the overlapping range of C isotopic composition with meteoritic nanodiamonds; the high concentrations of planar defect lamellae consistent with shock metamorphism; the radiation damage possibly due to cosmic ray exposure; the high porosity suggestive of loss of H gained by solar implantation; the age (2.6–3.8 Ga); the restricted distribution of carbonado; and their melt-like surfaces with globules, dimples, and furrows ('reticulate cantaloupe skin-like network').

Our report describes an investigation of the magnetic properties of carbonados and the nature of the magnetic components. Carbonados are commonly intergrown with hematite, magnetite, ilmenite, and chromite [2,19,24,25]. In addition, the diamond matrix contains small amounts of the uncommon metallic particles α-Fe, Ni, Cr, Fe–Mn, Ti, SiC, and taenite γ-(Fe, Ni) [19,22], thought to be related to an early reducing stage of their history. α-Fe and γ-(Fe, Ni) are the most abundant of these particles [19]. All other inclusions, outside the carbonado matrix, reside mainly in open pore space, and are thought to be of secondary origin [19].

Collinson [26] conducted a study of the magnetic properties of polycrystalline diamonds including carbonados from Brazil and the CAR. He reported that, in comparison to other diamonds, carbonados have very little magnetic material resulting in low magnetic intensities. The natural remanent magnetization (NRM) intensity ($(1–10)\times10^{-5}$ A m^2 kg^{-1}) was stable with a very small decrease ($\sim$10%) after demagnetization to 100 mT. These NRM directions showed a steady migration to stable primary end-points with irregular intensity decay curves. Conventional thermomagnetic experiments utilized to determine Curie points indicate a discontinuity at 120–160°C for some carbonados suggesting a Curie point, which has not been identified with a mineral species [26]. The initial magnetic susceptibility was $\sim5\times10^{-8}$ m^3 kg^{-1}. During isothermal remanent magnetization (IRM) acquisition, there were no indications of saturation up to an applied field of 800 mT. The REM ratio (NRM/saturation isothermal remanent magnetization (SIRM) is 0.1–0.01 as opposed to the range of terrestrial material, which is typically 0.01–0.001 [27].

Collinson [26] characterized the magnetic properties of the bulk carbonados. We, however, have investigated whether or not the magnetic carriers were distributed homogeneously throughout the diamond matrix. This distribution may constrain the history of carbonados.

2. Materials and methods

We recently obtained 20 carbonados from the CAR of variable size, color and morphology (Fig. 1). These samples possess diverse pore sizes and pore concentration, both of which decrease on glassy smooth surfaces (e.g. D10, D11, and D12, Fig. 1). All samples were subjected to ultrasound cleaning in water before measurements. NRM and SIRM were measured with a superconducting rock magnetometer, (SRM, Superconducting Technology). Hysteresis properties of strongly magnetic samples were measured with a vibrating sample magnetometer (VSM, Lake Shore *model 7300*). Magnetic fields of up to 2 T were supplied via a large, water-cooled, 12-inch Varian magnet, driven by a Tidewater bipolar power supply. All samples were further examined by optical and scanning electron microscopy (SEM).

For the purpose of reliable monitoring of the

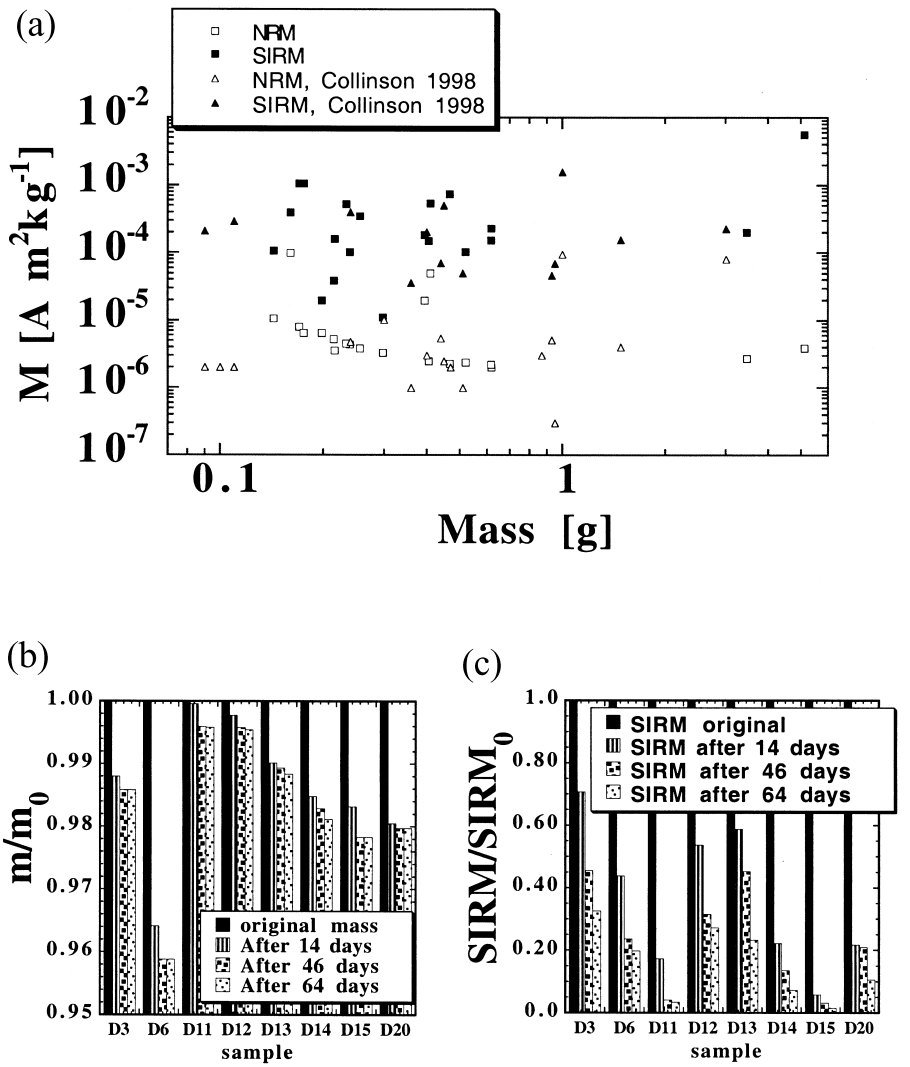

Fig. 2. (a) NRM and SIRM of carbonados from this and the Collinson (1998) study. (b) Mass (m = mass, m_0 = initial mass). (c) SIRM loss due to acid treatment ($SIRM_0$ = initial SIRM).

loss of magnetization during the acid treatment, only samples with large magnetic signatures were soaked in a 50:50 mixture of 50 wt% HF and 6 N HNO_3 for 24 h to remove surface contamination. Samples were then further soaked in 6 N HCl, which was removed every 72 h. Samples were washed and ultrasonically cleaned in water before the acid treatment renewed. In addition they were ultrasonically agitated while sitting in acid on a daily basis to promote dissolution. Mass and SIRM, acquired after each acid treatment in the direction fixed within the sample's coordination system, were measured after 14, 46, and 64 days. After 64 days, samples continued to dissolve in HCl as indicated by the yellow coloration of the acid towards the end of the 72 h cycle. However, at this stage, the magnetic signature was found to have dropped significantly as the acid penetrated into the pores and dissolved the magnetic minerals.

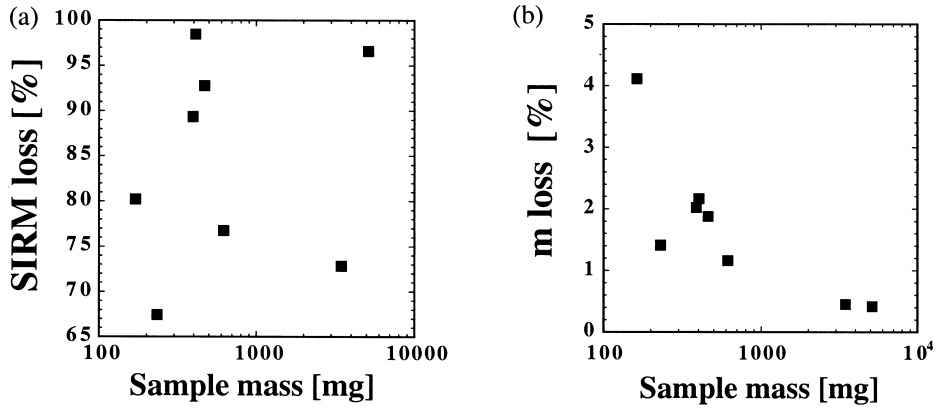

Fig. 3. Effect of acid treatment on saturation isothermal magnetization (SIRM) and mass (m). (a) SIRM fraction lost due to acid does not depend on the sample's mass. (b) Fraction of m removed due to acid decreases with the sample's mass.

3. Results

Fig. 2a compares measurements of the bulk magnetic properties of our untreated samples cleaned with ultrasound with the earlier work by Collinson [26]. Acid etching resulted in both loss of mass (Fig. 2b) and saturation remanence (Fig. 2c). A larger proportion of the magnetic signal was lost compared to the fractional mass loss. The extent of the magnetization loss (60–99% of initial SIRM) was essentially independent of the mass (Fig. 3a). However, the mass loss (1–5%) decreased with the increasing sample's original mass. (Fig. 3b).

Continuous acid treatment produced contrasting magnetic behavior in different samples. The treatment resulted in magnetic hardening (coercivity increases) in D-11 and D-15 (Fig. 4). Samples D-3 and D-6 show constant resistance to the AF (alternating magnetic field) demagnetization during all dissolution steps (Fig. 5). Acid treatment of samples D-12, D-13, D-14 and D-20 left magnetization carriers that had softer resistance against the AF field than before treatment (Fig. 6).

The etching-dependent magnetic signature reveals part of the carbonado post-formational history. With respect to the hysteresis loops (Fig. 7), it is clear that the nature of magnetic particles is bimodal and represents the combination of hard and soft magnetic material. This often results in constricted hysteresis loops. The resistance of magnetic remanence to an AF is rather large (Figs. 4–6). The effect of etching on the magnetic resistance against the (AF) demagnetization field is rather variable and echoes the oxide origin history of individual carbonados. Two carbonados

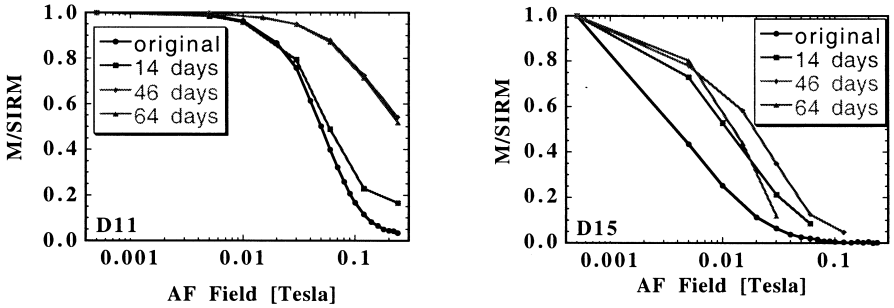

Fig. 4. Magnetization (M) behavior during the demagnetization of SIRM by an AF of D11 and D15 during the coarse of acid treatment.

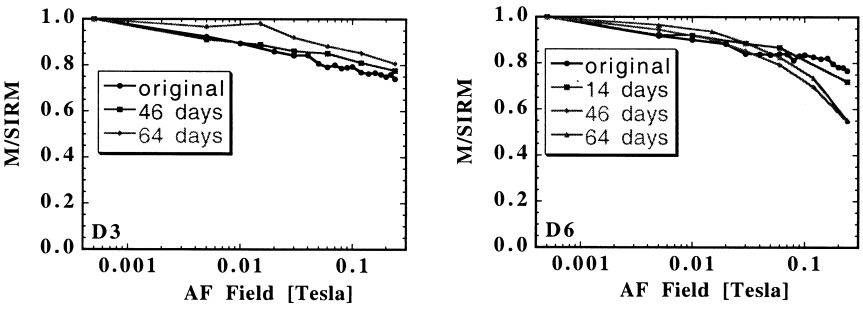

Fig. 5. Magnetization (M) behavior during the demagnetization of SIRM by an AF of D3 and D6 during the coarse of acid treatment.

(D-11 and D-15) experienced shift from low to high magnetic coercivity upon acid treatment (Fig. 4) characterized by an increase in resistance against the AF. These are the samples that lost more than 95% of their original saturation remanence. For these carbonados, detection of the carriers with large magnetic coercivity indicates that they are likely to be more primitive and that we must have at least two precipitation phases for the magnetic carries. Samples D-3 and D-6 retained constant magnetic resistance during the acid treatment suggesting that their magnetic mineralogy did not change in the course of etching (Fig. 5). This points to the genesis of a single magnetic phase. Samples characterized by constricted hysteresis loops (D-12, D-13, D-14, and D-20) revealed carriers with low coercivity sealed under the carriers with large magnetic coercivity (Fig. 6).

Table 1 summarizes the magnetic characteristics of our samples before acid treatment. NRM values were $(0.1–10)\times10^{-5}$ A m^2 kg^{-1}. This is consistent with measurements by Collinson [26] who

Table 1
Bulk magnetic properties of carbonados

Sample	Weight (mg)	NRM$\times10^{-6}$ (A m^2 kg^{-1})	SIRM$\times10^{-6}$ (A m^2 kg^{-1})	REM	H_c (mT)	J_s (A m^2 kg^{-1})
D1	238	4	101	0.043	20	0.0002
D2	143	11	107	0.099		0.0002
D3	233	5	524	0.0086		
D5	214	5	39	0.14		0.0001
D4	160	99	393	0.25	1.5	0.0057
D6	170	8	1070	0.0075		
D7	255	4	352	0.011		
D8	197	7	20	0.33		
D9	215	4	159	0.022	50	0.0004
D10	175	6	107	0.0061		
D11	5120	4	561	0.0007	31	0.0105
D12	3460	3	200	0.014	100	0.0002
D13	619	2	230	0.0087		
D14	467	2	736	0.0031	100	0.0015
D15	410	49	542	0.091	0.5	0.012
D16	617	2	154	0.014		
D17	520	2	104	0.023		
D18	298	3	11	0.29		
D19	405	2	151	0.017		
D20	395	20	183	0.11		0.0003

REM = NRM/SIRM, H_c = magnetic coercivity, J_s = saturation magnetization. Empty space indicates that the measured parameter was below the detection limit.

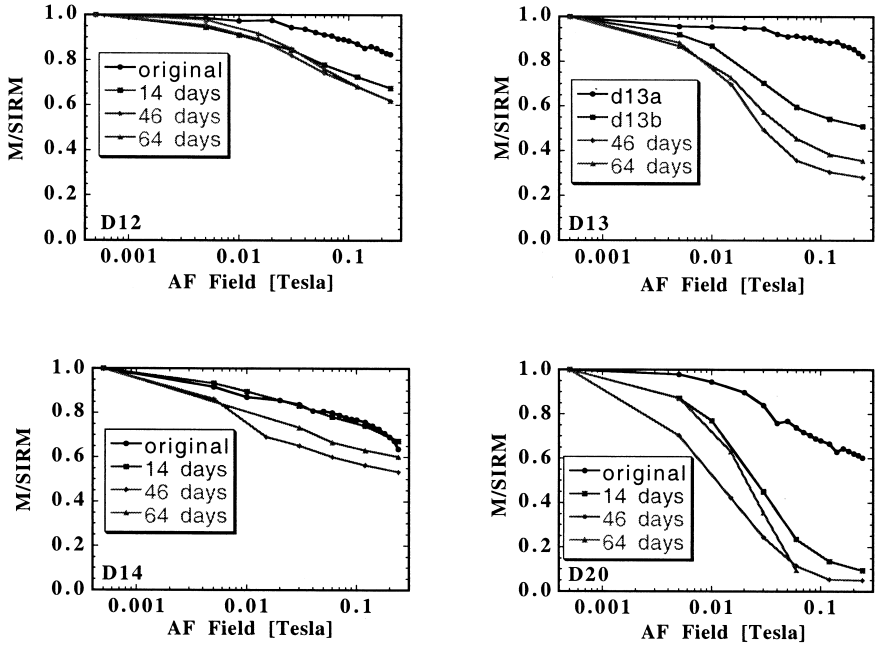

Fig. 6. Magnetization (M) behavior during the demagnetization of SIRM by an AF of D12, D13, D14 and D20 during the coarse of acid treatment.

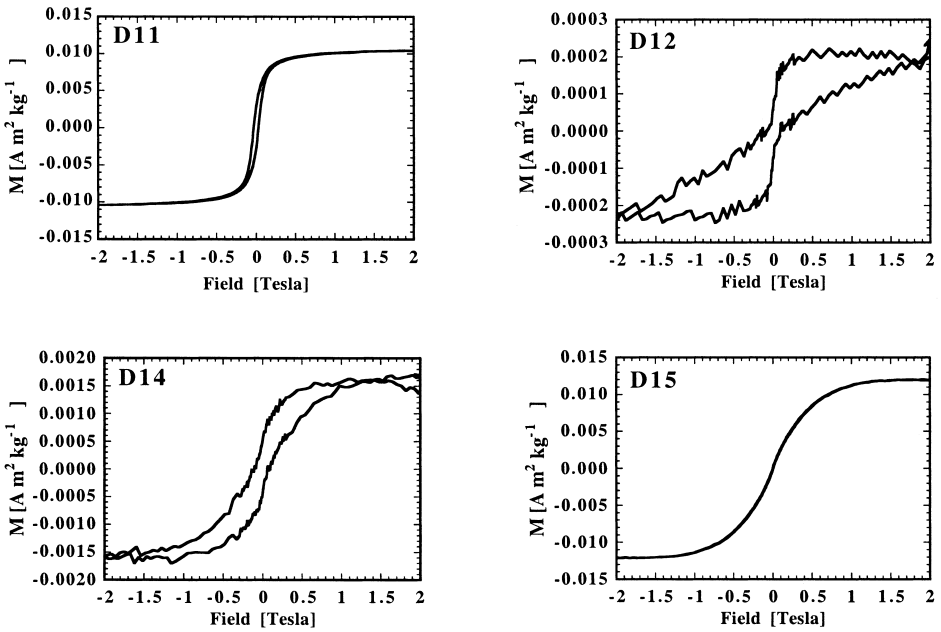

Fig. 7. Hysteresis loops of carbonados (M = magnetization). Sample D11 saturates in low fields (0.3 T). Hysteresis loops for samples D12 and D14 have constricted shape. Hysteresis loop for sample D15 saturates in high fields (0.8 T) and has low magnetic coercivity. All loops were corrected for diamagnetic slope (approximately -2×10^{-8} m^3 kg^{-1}) due to diamond host.

reported the same range of NRM values (see Fig. 2a). Saturation magnetization was in the range $(1.0–500)\times10^{-5}$ A m^2 kg^{-1} and REM ratios were 0.001–0.3. These hysteresis parameters were measured only on a limited number of samples due to the lower sensitivity of the VSM. Hysteresis loops were often constricted, indicating the presence of two magnetic components with different coercivity (see Fig. 7, samples D12 and D14). One loop (sample D-15 in Fig. 7) resembles native iron based on the large saturation field. All of the samples displayed a diamagnetic component $(-2.02\pm1.20)\times10^{8}$ m^3 kg^{-1} owing to the presence of the diamond matrix.

SEM observations have established two different morphologies of carbonados. The fresh broken surface (Fig. 8a) shows the porous nature of the polycrystalline matrix. The glassy-like texture (Fig. 8b) generally has a lower density of pores and large smooth surfaces. Before the acid treatment, pores contained variable amounts of minerals. Minerals species were uniform within individual samples but differed in between the samples based on energy dispersion X-ray (EDX) analyses. Elements contained in pores (O, Na, Al, Si, P, Cl, K, Ca, Ti, V and Fe) indicate a large variety of possible mineral species. Iron-containing minerals (Fig. 9) probably carry the observed magnetic signature. After the acid etching, SEM analysis confirmed that the previously filled pores were empty.

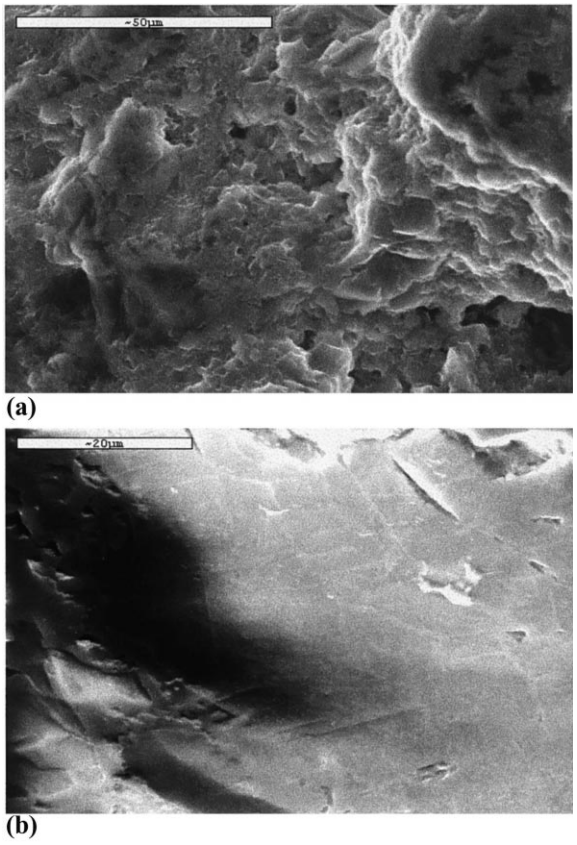

Fig. 8. Modes of physical characteristic of the carbonado surface: (a) An internal (fresh)surface of carbonado D7. (b) A smooth glassy carbonado surface (D1).

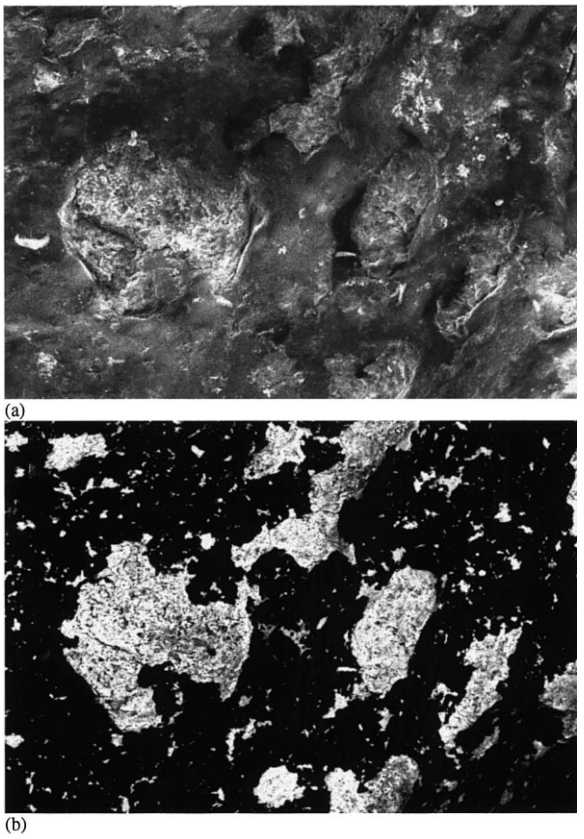

Fig. 9. Example of the iron oxide mineral concentrated within the pores of carbonado D11. The images are 50 μm wide. (a) Scanning electron image. (b) Back-scattered electron image of the same area as (a). The bright pore fill is composed of iron oxides

4. Discussion

The most significant results we report are the independence of the magnetic properties on the mass of carbonados and the observation that most of the magnetization is lost following acid treatment. If the magnetic carriers were distributed homogeneously throughout the sample, then larger samples would lose a smaller component of magnetization (normalized by mass) than smaller grains due to their lower surface-area-to-volume ratios. However, we do not see such a decrease. Instead, we note rather chaotic behavior, which we interpret as evidence that the magnetic carriers are not distributed homogeneously throughout the sample but are located on the surface. This is supported by the large magnitude of magnetization loss during the acid treatment. Since we ultrasonically cleaned these samples before etching in order to avoid surface contamination, the magnetic carriers may be part of the original, smooth surface and exposed pores of the carbonado. However, the interior (including the sealed pores), which was not exposed to the acid and is therefore unrelated to the smooth surface, is relatively free of magnetic carriers. According to our detection limit for hysteresis parameters, the mass concentration of metallic Fe particles (saturation magnetization = 218 A m^2 kg^{-1}) must be less than 10^{-5} wt%. Thus, there may still be room for a very limited concentration of small inclusions of metallic components within the carbonado matrix [19,22].

Our results suggest that the initial carbonado-forming episode must have taken place in an environment relatively free of magnetic materials. This event included the process of fusing the individual diamond subcrystals into an aggregate and the formation of their bulk porous matrix. Apart from a possible metallic (Fe) content of up to 10^{-5} wt%, the absence of internal magnetic materials has to be incorporated in the possible models of carbonado origin.

Mantle carbonado origin [16,17] necessitates that crustal organic matter, relatively free of iron bearing phases, could have been subducted into the mantle and converted to diamond, thereby explaining the light C isotopic signatures and high concentration of PAH species present [8,16]. If carbonados were formed in the mantle, in keeping with this model, one would expect them to be found in the vicinities of ancient subduction zones. Carbonados in sensu stricto, however, have yet to be recovered from outside Brazil and the CAR [24,25]. Furthermore, the high porosity exhibited by carbonados is difficult to interpret if they formed under conventional high-pressure mantle conditions [4]. Indeed, laser-induced luminescence indicates formation temperatures < 400°C [16,28].

The radiogenic fission origin requires that U and Th in carbonaceous matter can form at least the initial 'seeds' for the growth of the carbonados, in an environment free of magnetic carriers, under low-pressure conditions [7,12,29]. However, in order to further continue diamond growth, another diamond-forming process (perhaps a meteorite impact) must be invoked due to the inefficient mass transport mechanism associated with carbonado formation by irradiation [29].

Meteorite impacts in C-rich sediment have been proposed as another mechanism for carbonado formation [21,30]. During such impacts, organic matter or graphite nodules can be converted to diamond by shock metamorphism. If microdiamonds were part of the original meteorite, they might have served as useful nucleation centers [31]. The impact of a large extraterrestrial bolide is a highly energetic phenomenon that causes ejection, melting and vaporization of both target rocks and the projectile. Hypervelocity fragments ejected from the impact crater can travel through the air with velocities several times greater than that of the impacting projectile [32] and, as a consequence, may have experienced much greater relative aerodynamic effects resulting in a partial fusion of the carbonados' surface. Thus, the impact hypothesis cannot only explain the light C isotope ratios but also the common inclusions of crustal minerals within the carbonado pores. Our magnetic data suggests that the organic matter was free of magnetic carriers prior to such an impact. Tektites are formed by a bolide impacting a silica-rich target and commonly contain significant amounts of magnetic material [33]. Organic matter, however, can accumulate significant amounts

of C with minuscule amounts of magnetic carriers. We stress that the impact model is a viable mechanism. In addition, non-aggregated microdiamonds are associated with several other known impact sites (e.g. Popogai and Ries craters) [34–40].

One important characteristic of carbonados is the abundance of pores, which contain up to 0.3 wt% of organic matter [14]. The extracted C in this organic fraction is isotopically heavier ($\delta^{13}C = -25.2‰$) compared to C remaining as diamond matrix after extraction ($\delta^{13}C < -28‰$) and contains PAHs up to 0.002–0.004 wt% of carbonado [5]. Thus, organic compounds other than PAHs dominate the organic content of carbonados. However, because the fraction of PAHs increases with the decreasing grain size of crushed carbonado powder [5], it is inferred that these aromatic compounds were primarily resident within the closed pores of carbonados. The mean size of the diamond powder was much larger than that of the crystallites making up the carbonado and hence the actual content of PAHs in carbonado is likely to exceed the observed 0.002–0.004 wt% [5].

We propose that at least three distinct phases were involved in the formation of carbonados. **Phase one** was the formation of the PAHs. **Phase two** was the nucleation of the isolated euhedral crystals (~ 1 μm), with the possible incorporation of an abundant noble gas content. These crystals form the interior of carbonados with the abundant pore space (Fig. 8a) that trapped PAHs and/or noble gas content. Both of these phases occurred in the relative absence of magnetic carriers with the exception of metallic impurities, which did not exceed 10^{-5}%. **Phase three** was the formation of the vitreous, smooth surface (see Fig. 8b), which resembles a fusion crust. The mechanism for this surface genesis is unknown but is most likely related to the formation of most of the magnetic particles within the exposed pores (Fig. 9a,b). These particles are responsible for the magnetic signature of carbonados and are related to secondary precipitation during their residence time in the bedrock.

We thus associate formation of the majority of the magnetic carriers with the origin of the smooth surface. This may have occurred during the residence time in the Earth's crust via erosional forces associated with formation of crustal magnetic material within the carbonado pores. An alternative scenario is that the smooth, glassy patina is a fusion crust, formed perhaps during the ejection of carbonados into the Earth's atmosphere following their formation during the impact of a meteorite into C-rich sediment. Carbonados partially ablated due to hypervelocity contact with the Earth's early, O-poor atmosphere. This partial ablation resulted in a fusion of the originally porous material and a decrease in the original pore density. The remaining pores were filled by secondary mineralization of the impact-generated melt and/or later diagenetic processes. This process necessitates the accumulation of pure C in some form of organic-rich sediment early in the Earth's history (2.6–3.8 Ga).

We do not exclude the possibility that carbonados could be the impactor itself [4] and could have formed in an interstellar environment, perhaps in the wake of a supernova explosion. In this case, the formation of PAHs inside the pore space also needs to be placed in an interstellar environment.

However, magnetic carriers are formed in both cases after the smooth surface is formed, most likely in a terrestrial environment. They possess a variety of magnetic components, which allows one to split carbonados into the three magnetic groups, characterizing most likely, the magnetic-oxide precipitation history of the surrounding material. **Group 1** describes carbonados in which magnetic carriers with large coercivity were formed first deep in the pore space. These magnetic grains were isolated with the next generation of grains with much lower magnetic coercivity. **Group 2** describes samples in which the open pores are filled only with the magnetic carriers that have high coercivity and are evenly distributed in the pore space. **Group 3** describes carbonados in which the deep pores are filled with magnetic carriers with low coercivity. These carriers are isolated later with material containing magnetic carriers that have relatively large magnetic coercivity.

5. Conclusions

1. The independence of magnetization on carbonado mass and the fact that a significant amount of this magnetization was lost during the acid treatment indicate that most of the magnetic material is located in pores with direct access to the sample surface.
2. The formation of the major magnetic component is either contemporaneous with that of the surface or the result of a later event.
3. The saturation–remanence dependence on the etching indicates that the magnetic properties have more- and less-primitive magnetic components with distinct coercivity. This probably relates to the environmental history of individual carbonado grains during their residence period in the terrestrial crust.
4. Our findings are consistent with carbonado formation associated with a meteorite impact where C-rich matter is either the 'target' or the 'bullet'.

Acknowledgements

This work was conducted while G.K. and H.G.M.H. were NAS/NRC Resident Research Associates at NASA, GSFC. We thank to Dr. Joseph A. Nuth, III for valuable and enlightening discussions and to Drs. Chris Koeberl, Stephen Haggerty and David Collinson for their scrupulous and constructive reviews of our manuscript.*[RV]*

References

[1] S.E. Haggerty, A diamond trilogy: superplumes, supercontinents, and supernovae, Science 285 (1999) 851–860.
[2] L.F. Trueb, E.C. de Wys, Carbon from Ubangi – A microstructural study, Am Mineral. 59 (1971) 1252–1268.
[3] F.V. Kaminskii, S.I. Kirikilitsa, G.K. Eremenko, I.A. Polkanov, A.J. Khrenov, New data on Brazilian carbonado, Dokl. Akad. Nauk SSSR 249 (1979) 443–445.
[4] S.E. Haggerty, Diamond–carbonado: Geological implications and research-industrial applications, Proceedings of the 5th NIRIM International Symposium on Advanced Materials (1998) 39–42.
[5] F.V. Kaminskii, I.I. Kulakova, A.I. Ogloblina, Polycyclic aromatic-hydrocarbons in carbonado and diamond, Dokl. Akad. Nauk SSSR 283 (1985) 985–988.
[6] C.R. Scotese, A.J. Boucot, W.S. McKerrow, Gondwanan palaeogeography and palaeoclimatology, J. Afr. Earth Sci. 28 (1999) 99–114.
[7] M. Ozima, M. Tatsumoto, Radiation-induced diamond crystallization Origin of carbonados and its implications on meteorite nano-diamonds, Geochim. Cosmochim. Acta 61 (1997) 369–376.
[8] D.N. Robinson, The characteristics of natural diamond and their interpretation, Mineral. Sci. Eng. 10 (1978) 55–72.
[9] H. Kamioka, K. Shibata, I. Kajizuka, T. Ohta, Rare-earth element patterns and carbon isotopic composition of carbonados implications for their crustal origin, Geochem. J. 30 (1996) 189–194.
[10] R. Burgess, L.H. Johnson, D.P. Mattey, J.W. Harris, G. Turner, He, Ar and C isotopes in coated and polycrystalline diamonds, Chem. Geol. 146 (1998) 205–217.
[11] K. Shibata, H. Kamioka, F.V. Kaminskii, V.I. Koptil, Rare earth element patterns of carbonado and yakutite evidence for their crustal origin, Mineral. Mag. 57 (1993) 607–611.
[12] M. Ozima, S. Zashu, K. Tomura, Y. Matsuhisa, Constraints from noble-gas content on the origin of carbonado diamonds, Nature 351 (1991) 472–474.
[13] S. Zashu, H. Hiyagon, Degassing mechanisms of noble gases from carbonado diamonds, Geochim. Cosmochim. Acta 59 (1995) 1321–1328.
[14] E.M. Galimov, F.V. Kaminskii, L.A. Kodina, New data on isotopic composition of carbon in carbonado, Geokhimiya 5 (1985) 723–726.
[15] F.V. Kaminskii, Origin of polycrystalline carbonado diamond aggregates, Dokl. Akad. Nauk. SSSR 294, 1987.
[16] H. Kagi, K. Takahashi, H. Hidaka, A. Masuda, Chemical properties of Central African carbonado and its genetic implications, Geochim. Cosmochim. Acta 58 (1994) 2629–2638.
[17] A.I. Gorshkov, L.V. Bershov, S.F. Vinokurov, K.L. Oton, A.V. Sivtsov, A.V. Mokhov, E.O. Bogacheva, Carbonado from the Lenkoish region, Bahia State (Brazil) mineral inclusions, physical properties, geochemical features, and formation conditions, Geol. Ore Depos. 39 (1997) 229–236.
[18] D. Shelkov, A.B. Verhovsky, H.J. Milledge, C.T. Pillinger, Carbonado A comparison between Brazilian and Ubangui sources with other forms of microcrystalline diamond based on carbon and nitrogen isotopes, Geol. Geofiz. 38 (1997) 315–322.
[19] A.I. Gorshkov, S.V. Titkov, A.M. Pleshakov, A.V. Sivtsov, L.V. Bershov, Inclusions of native metals and other mineral phases into carbonado from the Ubangi region (Central Africa), Geol. Ore Depos. 38 (1996) 114–119.
[20] F.V. Kaminskii, Y.A. Klyuyev, B.I. Prokopchuk, S.A. Shekeka, V.I. Smirnov, I.N. Ivanovskaya, First carbonado and new ballas find in the Soviet Union, Akad. Nauk SSSR Dokl. Earth Sci. Sect. 242 (1978) 152–155.

[21] J.V. Smith, J.B. Dawson, Carbonado Diamond aggregates from early impacts of crustal rocks?, Geology 13 (1985) 342–343.
[22] S. De, P.J. Heaney, R.B. Hargraves, E.P. Vicenzi, P.T. Taylor, Microstructural observations of polycrystalline diamond A contribution to the carbonado conundrum, Earth Planet. Sci. Lett. 164 (1998) 421–433.
[23] I.L. Orlov, F.V. Kaminskii, Carbonado with lonsdaleite – A new (IX) variety of polycrystalline aggregate of diamond, Dokl. Akad. Nauk SSSR 259 (1981) 459–461.
[24] L.F. Trueb, W.C. Butterman, Carbonado: A microstructural study, Am. Mineral. 54 (1969) 412–425.
[25] L.F. Trueb, E.C. de Wys, Carbonado natural polycrystalline diamond, Science 165 (1969) 799–802.
[26] D.W. Collinson, Magnetic properties of polycrystalline diamonds, Earth Planet. Sci. Lett. 161 (1998) 179–188.
[27] P.J. Wasilewski, Magnetic and microstructural properties of some lodestones, Phys. Earth Planet. Inter. 15 (1977) 349–362.
[28] H. Kagi, A. Masuda, Laser-induced luminescence from natural polycrystal diamond, carbonado – a new possible thermal indicator of meteoritic diamonds, Naturwissenschaften 78 (1991) 335–358.
[29] T.L. Daulton, M. Ozima, Radiation-induced diamond formation in uranium-rich carbonaceous materials, Science 271 (1996) 1260–1263.
[30] V.A. Yezerskiy, High pressure polymorphs produced by the shock transformation of coals, Intl. Geol. Rev. 28 (1986) 221–228.
[31] S.E. Haggerty, Diamond–carbonado models for a new meteorite class of circumstellar or solar system origin, Eos 77 (1996) S143.
[32] H.J. Melosh, Cratering mechanics – observational, experimental, experimental, and theoretical, Annu. Rev. Earth Planet. Sci. 8 (1980) 65–93.
[33] A.N. Thorpe, F.E. Senftle, L. May, A. Barkatta, M.A. Adelhadadi, G.S. Marbury, G.A. Izett, F.R. Maurrasse, Comparison of the magnetic properties and Mössbauer analysis from the Cretaceous–Tertiary boundary, Beloc, Haiti, with tektites, J. Geophys. Res. Lett. – Planets 99 (1994) 10881–10886.
[34] A. ElGoresy, G. Donnay, A new allotropic form of carbon from the Ries crater, Science 161 (1968) 363–364.
[35] R.E. Hanneman, H.M. Strong, F.P. Bundy, Hexagonal diamonds in meteorites; implications, Science 155 (1967) 995–997.
[36] A.R. Hildebrand, G.T. Penfield, D.A. Kring, M. Pilkington, Z.N. Camargo, S.B. Jacobsen, W.V. Boynton, Chicxulub crater; a possible Cretaceous/Tertiary boundary impact crater on the Yucatan Peninsula, Mexico, Geology 19 (1991) 867–871.
[37] C.C. Swisher, J.M.N. Grajales, A. Montanari, S.V. Margolis, P. Claeys, W. Alvarez, P.R. Renne, P.E. Cedillo, J.M.R.F. Maurrasse, H.G. Curtis, J. Smit, M.O. McWilliams, Coeval ($^{40}Ar/^{39}Ar$) ages of 65.0 million years ago from Chicxulub Crater melt rock and Cretaceous–Tertiary boundary tektites, Science 257 (1992) 954–958.
[38] P.S. DeCarli, Shock wave synthesis of diamond and other phases, Mat. Res. Soc. Symp. Proc. 383 (1995) 21–31.
[39] R.M. Hough, I. Gilmour, C.T. Pillinger, J.W. Arden, R.W.R. Gilkes, J. Yuan, H.J. Milledge, Diamonds and silicon carbide in impact melt rock from the Ries impact crater, Nature 378 (1995) 41–44.
[40] C. Koeberl, V.L. Masaitis, G.I. Shafranovsky, M. Schrauder, I. Gilmour, F. Langenhorst, Diamonds from the Popoigai impact structure, Russia, Geology 25 (1997) 967–970.